Ultralow-threshold Raman laser using a spherical dielectric microcavity

S. M. Spillane, T. J. Kippenberg & K. J. Vahala

Department of Applied Physics, California Institute of Technology, Pasadena, California 91125, USA

The ability to confine and store optical energy in small volumes has implications in fields ranging from cavity quantum electrodynamics to photonics. Of all cavity geometries, micrometre-sized dielectric spherical resonators are the best in terms of their ability to store energy for long periods of time within small volumes[1]. In the sphere, light orbits near the surface, where long confinement times (high Q) effectively wrap a large interaction distance into a tiny volume. This characteristic makes such resonators uniquely suited for studies of nonlinear coupling of light with matter. Early work[2,3] recognized these attributes through Raman excitation in microdroplets—but microdroplets have not been used in practical applications. Here we demonstrate a micrometre-scale, nonlinear Raman source that has a highly efficient pump–signal conversion (higher than 35%) and pump thresholds nearly 1,000 times lower than shown before. This represents a route to compact, ultralow-threshold sources for numerous wavelength bands that are usually difficult to access. Equally important, this system can provide a compact and simple building block for studying nonlinear optical effects and the quantum aspects of light.

Raman sources based on silica may be helpful in extending the available range of semiconductor lasers. But to date these sources have required very high pump power, and are macroscale devices. Silica microspheres are good candidates for next-generation Raman sources, and have the highest *Q*-factors (quality factors) of any optical resonator ($>10^9$). Here we report a Raman source consisting of a high-*Q* silica microsphere coupled to an optical fibre. This device enables a large reduction in the necessary threshold pump power[4], while fibre-coupling[5] notably improves overall efficiency and provides a convenient method of optical field transport. Although a single Raman laser is investigated in this work, the ability to fibre-couple should enable easy scaling to multiple resonant systems along a single fibre (Fig. 1).

The lasing threshold occurs when cavity round-trip gain equals round-trip loss. For an intensity-dependent gain coefficient (such as for a Raman laser), and taking into account the power build-up factor in a resonator, we obtain the following equation for threshold pump power;

$$P_{\text{threshold}} = \frac{\pi^2 n^2}{\lambda_P \lambda_R} \frac{V_{\text{eff}}}{\Gamma B g} Q_e^P \left(\frac{1}{Q_T^P}\right)^2 \frac{1}{Q_T^R} \qquad (1)$$

Here $P_{\text{threshold}}$ denotes the incident power necessary in the fibre (not the power coupled into the resonator), n is the index of refraction, V_{eff} is the effective pump mode volume (that is, taking the full-width at half-maximum of the intensity distribution), λ_P and λ_R are the pump and Raman wavelengths, Γ is the spatial mode overlap factor between pump and Raman modes ($\Gamma \approx 1$), g is the nonlinear bulk Raman gain coefficient, B is a correction factor of the circulating power due to internal backscattering (between 1 and 0.5), and Q_T^P is the total quality factor for the pump mode, made up of an intrinsic contribution Q_o^P and a coupling contribution Q_e^P (and similarly for the Raman mode). Equation (1) has the important feature that the threshold pump power scales inversely with the factor Q^2/V, which is the same as quality factor multiplied by the cavity Purcell factor ($\propto Q/V$). Thus quality factor plays a dominant role in device performance, resulting from the necessity of a doubly resonant process. This is a classical conclusion, neglecting the additional benefit due to enhancement of the gain coefficient by cavity quantum electrodynamics[6] (QED).

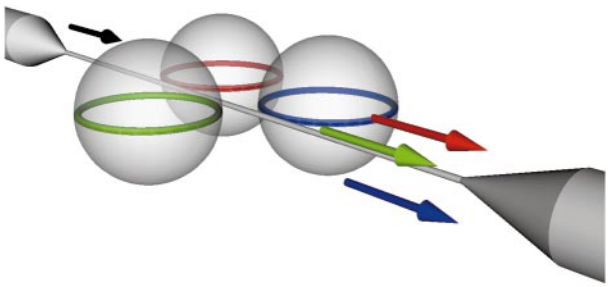

Figure 1 Cascading multiple Raman lasers along a single fibre. Black arrow represents input wave. Each microsphere may emit a different Raman wave, indicated by the coloured arrows.

Silica microspheres were fabricated by melting the tip of a standard telecommunication (SMF-28) fibre with a CO_2 laser; surface tension creates a spherical volume with low eccentricities (~2%). These spheres were optically coupled by the use of a tapered optical fibre, formed by heating and stretching a length of single-mode fibre. Typical taper diameters were approximately 1.5 μm with losses of less than 5%. Details of the fabrication of microspheres and tapers are given elsewhere[5]. A polarization controller was used to adjust the incident polarization state at the sphere–taper junction to maximize the coupling efficiencies while preserving large values of *Q*. In these measurements, values of *Q* were in the low 10^8 range, believed to be limited by surface scattering and OH absorption[7]. Surface scattering also induces backscattering of power and couples the initially degenerate clockwise and anti-clockwise circulating modes, causing a splitting of the resonance wavelength[8], in addition to a reduction of the circulating power (up to a factor of two). The taper position is controlled relative to the microsphere by a three-axis stage with a resolution of 20 nm. A tunable 1,550-nm external-cavity diode laser with 300-kHz linewidth is used as a pump. The laser is scanned repeatedly through a frequency range of approximately 60 GHz around a single whispering-gallery mode (WGM).

Figure 2 shows the emission spectrum for a Raman microsphere laser (intrinsic pump quality factor of $Q_o = 10^8$) excited far above the threshold for stimulated Raman scattering. There are a multi-

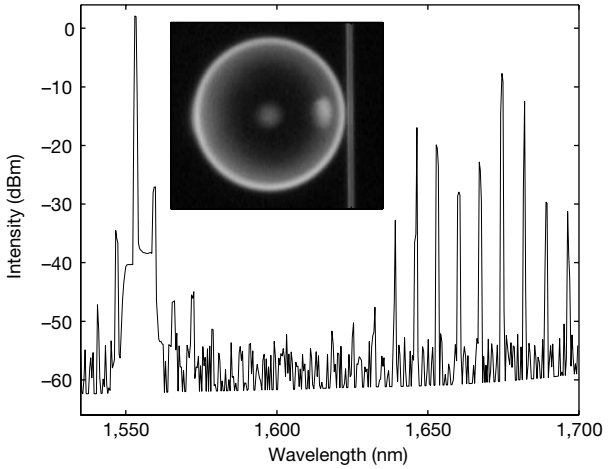

Figure 2 Spectrum of a 70-μm-diameter Raman microsphere laser with pump powers of 2 mW. The pump is at 1,555 nm. Peaks located around 1,670 nm are Raman oscillations, separated by the free spectral range of the microsphere. Secondary lines around 1,555 nm are due to four-wave mixing between the pump and two Raman waves. Inset, a microsphere coupled to a fibre taper.

Report Documentation Page

Form Approved
OMB No. 0704-0188

1. REPORT DATE	2. REPORT TYPE	3. DATES COVERED
01 JUN 2005	**N/A**	**-**

4. TITLE AND SUBTITLE	5a. CONTRACT NUMBER
Ultralow-threshold Raman laser using a spherical dielectric microcavity	5b. GRANT NUMBER
	5c. PROGRAM ELEMENT NUMBER
6. AUTHOR(S)	5d. PROJECT NUMBER
	5e. TASK NUMBER
	5f. WORK UNIT NUMBER
7. PERFORMING ORGANIZATION NAME(S) AND ADDRESS(ES) **Department of Applied Physics, California Institute of Technology, Pasadena, California 91125, USA**	8. PERFORMING ORGANIZATION REPORT NUMBER
9. SPONSORING/MONITORING AGENCY NAME(S) AND ADDRESS(ES)	10. SPONSOR/MONITOR'S ACRONYM(S)
	11. SPONSOR/MONITOR'S REPORT NUMBER(S)

12. DISTRIBUTION/AVAILABILITY STATEMENT
Approved for public release, distribution unlimited

13. SUPPLEMENTARY NOTES
See also ADM001923.

14. ABSTRACT

15. SUBJECT TERMS

16. SECURITY CLASSIFICATION OF:			17. LIMITATION OF ABSTRACT	18. NUMBER OF PAGES	19a. NAME OF RESPONSIBLE PERSON
a. REPORT	b. ABSTRACT	c. THIS PAGE			
unclassified	**unclassified**	**unclassified**	**UU**	**3**	

tude of nonlinearly generated wavelengths, from stimulated Raman peaks centred around 1,670 nm to Raman-assisted four-wave-mixing peaks located symmetrically about the 1,550-nm pump. Stimulated Raman scattering has a very high threshold (nonlinear gain coefficient of 10^{-11} cm W^{-1}), requiring significant circulating pump powers. This suggests that other nonlinear processes having lower thresholds, such as stimulated Brillouin scattering (SBS), could also be present in the systems tested. SBS, for example, should have a threshold roughly 500 times lower than stimulated Raman scattering (nonlinear gain coefficient is 500 times larger). To determine the presence of SBS, an optical spectrum analyser was used to measure backward-propagating optical power coupled from the microresonator into the fibre taper. The gain spectrum for SBS is very narrow (<100 MHz) with a roughly 10 GHz frequency down-shift in silica. The microresonators tested here have free spectral ranges on the order of terahertz, with an eccentricity splitting of the azimuthal modes on the gigahertz scale[9]. In general, this splitting is dependent upon fabrication-induced irregularities, thus overlap with the SBS spectrum is unlikely. Consequently, SBS was only observed when a WGM overlapped the Brillouin gain spectrum, in agreement with experiments on liquid droplets[10]. However, the backward spectral monitor did show the expected strong Raman oscillation. Cascaded Raman peaks, if present, were not observable due to the wavelength range of our optical spectrum analyser. We note that four-wave mixing associated with the Kerr effect was also observed. However, such processes in microcavities are governed by strict conditions imposed by the combined effect of the phase-matching requirement with the WGM spectral structure. This will be investigated in future work.

To investigate the dependence on quality factor, the threshold was measured while varying the coupling between the taper and microsphere by changing the air gap (Fig. 3). The data follow a near-parabolic shape, with a measured minimum value of 62 μW. This value is, to our knowledge, the lowest directly measured (not inferred) threshold for any nonlinear substance to date. A theoretical fit, based on exponential dependence of the coupling Q, shows excellent agreement. We also obtain good agreement with a calculated minimum threshold value of 50 μW under the assumption that Raman mode Q is equal to pump mode Q. The minimum threshold does not lie at the critical coupling point[11], where circulating pump power (Raman gain) is largest. It in fact occurs for the system in a slightly undercoupled state (weaker coupling than at the critical point), corresponding to an observed pump transmission of 12%. This shift results from the interplay between Raman gain and loss, caused by the coupling of both the pump and Raman wave to the fibre waveguide. In the simplified case where the quality factors of pump and oscillating modes are equal, the theoretical minimum occurs for a pump power transmission of 11%, in good agreement with the experimental value.

Examining the threshold equation (equation (1)), the threshold is expected to scale approximately as radius squared (effective mode volume is nearly quadratic in radius). To investigate this, the minimum threshold for various sphere diameters ranging from 28 to 110 μm was measured (Fig. 3 inset). The threshold indeed follows a quadratic dependence on size. The dependence on quality factor is normalized out (assuming pump and Raman Q are identical) due to its strong effect on threshold. In previous work on microdroplets, it was found that for droplets with diameters of less than 30 μm there is an additional threshold reduction due to cavity QED effects[12]. In the present work we could not accurately determine threshold in this size range. Smaller spheres experienced very large temperature effects, causing the WGMs to experience instabilities[13] as well as thermal shifting of the spectrum, complicating pumping of the resonant mode. With sufficient thermal control it may be possible to quantify precisely the reduction of threshold in this smaller size regime.

The efficiency of the Raman oscillator was investigated by decreasing the pump power until a single emission wavelength was observed on the optical spectrum analyser (Fig. 4). The measured threshold is 86 μW for this 40-μm sphere. This value is nearly 1,000 times lower than the corresponding values measured in previous work using microdroplets (45 mW for a 30-μm CS_2 droplet; ref. 11), despite the fact that silica has a 1,000 times smaller Raman gain coefficient. This improvement of nearly 10^6 results from efficient single WGM excitation, whereas free-space beams (used previously) lack high spatial mode selectivity. Upon closer examination, the Raman emission in fact consisted of a number of separate simultaneously oscillating peaks (to the temporal resolution of the optical spectrum analyser), corresponding to different azimuthal modes. The number of oscillating modes was typically 3–5, owing to the spatial selectivity of the fibre-taper. The measured unidirectional absolute conversion efficiency was 16%, with a differential quantum efficiency (clockwise and anticlockwise

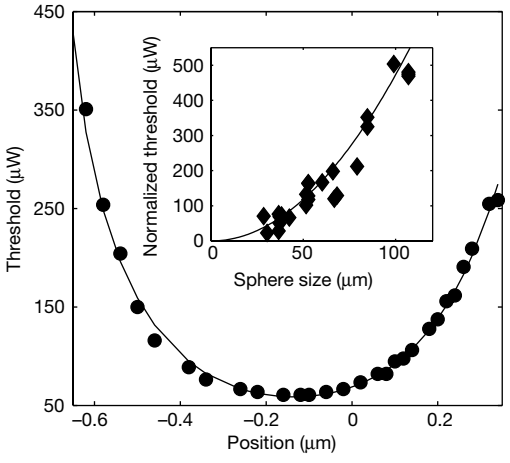

Figure 3 Coupling gap and size dependence of the Raman threshold. Main figure, Raman oscillation threshold versus taper–sphere gap for a 40-μm-diameter sphere ($Q_0 = 10^8$). Position is measured from the critical coupling point, and negative values correspond to the undercoupled regime. The minimum threshold occurs with the microsphere about 0.15 μm undercoupled, and corresponds to a transmission of 12%. Solid line, a theoretical fit to the threshold equation. Inset, normalized minimum threshold versus sphere size, which follows a quadratic dependence.

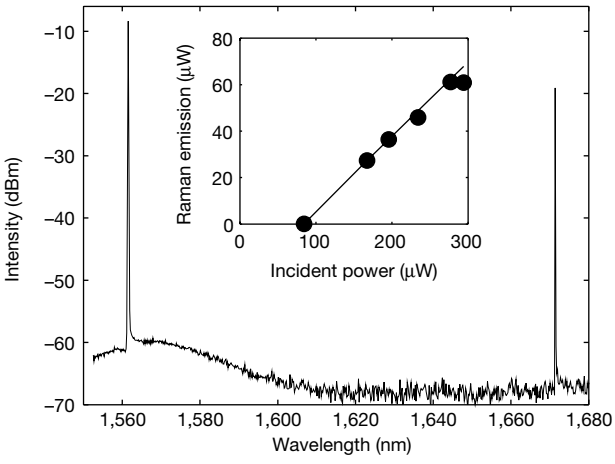

Figure 4 Single longitudinal mode Raman lasing. Raman spectrum for a 40-μm-diameter microsphere, exhibiting a unidirectional conversion efficiency of 16% (pump is at 1,555 nm). Inset, Raman power output (sum of forward and backward emission) versus incident pump power. Differential quantum efficiency is 36%.

oscillation) of 36%. In other microspheres tested, Raman output powers as large as 200 μW were obtained.

There are several ways to improve the performance of this system. Quality factors of 10^9 have been achieved previously in fused-silica microspheres[14], which should lead to submicrowatt Raman thresholds. The use of small spheres (provided temperature issues can be resolved) should improve Raman conversion efficiencies under increased pump power due to the increase in free spectral range, which decreases the efficiency of secondary Raman lines and Raman-assisted four-wave mixing. Disks should allow true single-mode emission. Concerning the outlook for future work and the implications of our work beyond an ultra-efficient and compact Raman source: there are several potential avenues that could be useful in fundamental studies. First, we note that opportunities exist to explore cavity QED effects in smaller microsphere samples[6]. As noted above, this will require an improvement in the stabilization of the sphere temperature. Additionally, the ability to achieve ultra-low-loss coupling between the resonator and the fibre taper suggests that compound resonant systems could be studied by attachment of multiple resonators along a single fibre taper. As noted earlier, we have observed Raman and SBS oscillation as well as four-wave mixing in these systems. These nonlinearities can be accessed in a compact volume through a nearly ideal field transport channel (optical fibre) and field coupling junction (the taper). As such, this system can be viewed more broadly as a building block for study of a host of nonlinearities within a high-*Q* silica resonator, and potentially for generation of non-classical photon states[15,16] and their efficient transport. Indeed, we believe the compact nature of the system combined with the power of fibre field transport could afford relatively straightforward access to single or tandem resonant systems in normally challenging environments such as ultralow-temperature chambers[17]. The ability to load or suitably modify spheres using dopants or quantum dots[18] could also be useful in such studies. □

Received 10 October; accepted 7 December 2001.

1. Collot, L., Lefevre-Seguin, V., Brune, M., Raimond, J. M. & Haroche, S. Very high-Q whispering-gallery mode resonances observed on fused silica microspheres. *Europhys. Lett.* **23,** 327–334 (1993).
2. Qian, S. X. & Chang, R. K. Multiorder Stokes emission from micrometer-size droplets. *Phys. Rev. Lett.* **56,** 926–929 (1986).
3. Lin, H. B., Huston, A. L., Eversole, J. D. & Campillo, A. J. Double-resonance stimulated Raman-scattering in micrometer-sized droplets. *J. Opt. Soc. Am. B* **7,** 2079–2089 (1990).
4. Braunstein, D., Khazanov, A. M., Koganov, G. A. & Shuker, R. Lowering of threshold conditions for nonlinear effects in a microsphere. *Phys. Rev. A* **53,** 3565–3572 (1996).
5. Knight, J. C., Cheung, G., Jacques, F. & Birks, T. A. Phase-matched excitation of whispering-gallery-mode resonances by a fiber taper. *Opt. Lett.* **22,** 1129–1131 (1997).
6. Chang, R. K. & Campillo, A. J. (eds) *Optical Processes in Microcavities* (World Scientific, Singapore, 1996).
7. Gorodetsky, M. L., Savchenkov, A. A. & Ilchenko, V. S. Ultimate Q of optical microsphere resonators. *Opt. Lett.* **21,** 453–455 (1996).
8. Weiss, D. S. *et al.* Splitting of high-Q Mie modes induced by light backscattering in silica microspheres. *Opt. Lett.* **20,** 1835–1837 (1995).
9. Lai, H. M., Leung, P. T., Young, K., Barber, P. W. & Hill, S. C. Time-independent perturbation for leaking electromagnetic modes in open systems with application to resonances in microdroplets. *Phys. Rev. A* **41,** 5187–5198 (1990).
10. Zhang, J. Z. & Chang, R. K. Generation and suppression of stimulated Brillouin scattering in single liquid droplets. *J. Opt. Soc. Am. B* **6,** 151–153 (1989).
11. Cai, M., Painter, O. & Vahala, K. J. Observation of critical coupling in a fiber taper to a silica-microsphere whispering-gallery mode system. *Phys. Rev. Lett.* **85,** 74–77 (2000).
12. Lin, H. B. & Campillo, A. J. CW nonlinear optics in droplet microcavities displaying enhanced gain. *Phys. Rev. Lett.* **73,** 2440–2443 (1994).
13. Ilchenko, V. S. & Gorodetskii, M. L. Thermal nonlinear effects in optical whispering gallery microresonators. *Laser Phys.* **2,** 1004–1009 (1992).
14. Vernooy, D. W., Ilchenko, V. S., Mabuchi, H., Steed, E. W. & Kimble, H. J. High-Q measurements of fused-silica microspheres in the near infrared. *Opt. Lett.* **23,** 247–249 (1998).
15. Bachor, H.-A., Levenson, M. D., Walls, D. F., Perlmutter, S. H. & Shelby, R. M. Quantum nondemolition measurements in an optical-fiber ring resonator. *Phys. Rev. A* **38,** 180–190 (1988).
16. Silberhorn, Ch. *et al.* Generation of continuous variable Einstein-Podolsky-Rosen entanglement via the Kerr nonlinearity in an optical fiber. *Phys. Rev. Lett.* **6,** 4267–4270 (2001).
17. Treussart, F. *et al.* Evidence of the intrinsic Kerr bistability of high-Q microsphere resonators in superfluid helium. *Eur. Phys. J. D* **1,** 235–238 (1998).
18. Fan, X., Palinginis, P., Lacey, S., Wang, H. & Lonergan, M. C. Coupling semiconductor nanocrystals to a fused-silica microsphere: a quantum-dot microcavity with extremely high Q factors. *Opt. Lett.* **25,** 1600–1602 (2000).

Acknowledgements

We thank A. D. Stone and R. K. Chang for comments. This work was supported by DARPA, NSF and the Caltech Lee Center.

Competing interests statement

The authors declare that they have no competing financial interests.

Correspondence and requests for materials should be addressed to K.J.V. (email: vahala@caltech.edu).

Observation of ligand effects during alkene hydrogenation catalysed by supported metal clusters

A. M. Argo, J. F. Odzak, F. S. Lai & B. C. Gates

Department of Chemical Engineering and Materials Science, University of California, Davis, California 95616, USA

Homogeneous organometallic catalysts and many enzymes activate reactants through coordination to metal atoms; that is, the reactants are turned into ligands and their reactivity controlled through other ligands in the metal's coordination sphere[1]. In the case of supported metal clusters, catalytic performance is influenced by the support and by adsorbed reactants, intermediates or products. The adsorbates are usually treated as ligands, whereas the influence of the supports is usually ascribed to electronic interactions[2,3], even though metal clusters supported on oxides[4–6] and zeolites[7] form chemical bonds to support oxygen atoms. Here we report direct observations of the structure of supported metal clusters consisting of four iridium atoms, and the identification of hydrocarbon ligands bound to them during propene hydrogenation. We find that propene and molecular hydrogen form propylidyne and hydride ligands, respectively[8], whereas simultaneous exposure of the reactants to the supported iridium cluster yields ligands that are reactive intermediates during the catalytic propane-formation reaction. These intermediates weaken the bonding within the tetrahedral iridium cluster and the interactions between the cluster and the support, while replacement of the MgO support with γ-Al_2O_3 boosts the catalytic activity tenfold, by affecting the bonding between the reactant-derived ligands and the cluster and therefore also the abundance of individual ligands. This interplay between the support and the reactant-derived ligands, whereby each influences the interaction of the metal cluster with the other, shows that the catalytic properties of supported metal catalysts can be tuned by careful choice of their supports.

Our Ir_4 clusters resemble the platinum nanoclusters in industrial naphtha reforming catalysts[9,10]. Decarbonylation of $[Ir_4(CO)_{12}]$ on porous γ-Al_2O_3 (surface area, 100 $m^2 g^{-1}$) or of $[HIr_4(CO)_{11}]^-$ on MgO (70 $m^2 g^{-1}$)[11,12] yielded supported Ir_4 catalyst samples with 1 wt% Ir that were used to catalyse the hydrogenation of ethene and propene. Conventional measurements of catalytic reaction rates[13] were complemented by extended X-ray absorption fine structure (EXAFS)[14] and infrared (IR)[8] spectroscopies, allowing us to determine the cluster structure and identify the ligands derived from the supports and the reactants while the catalysts were active in flow reactors. Infrared spectra of adsorbate ligands were determined by subtracting the spectrum of the sample in an inert gas (He) from that of the sample in the treatment gas; when absorption by the reactant gas or product gas was significant, its spectrum was also subtracted[8].